Null Quasi-Spherical Einstein characteristic code

Robert A. Bartnik (robert.bartnik@sci.monash.edu.au)

Andrew H. Norton (andrew.norton@uts.edu.au)

[1] website: `http://relativity.ise.canberra.edu.au`

[2] *Numerical methods for the Einstein equations in NQS coordinates*, SIAM J. Sci. Comp. 22 (2000), pp917-950.

The Null Quasi-Spherical ansatz

The NQS coordinates $(z, r, \vartheta, \varphi)$ satisfy:

- The 3-surfaces $z = const.$ are null,
- The 2-surfaces $(z, r) = const.$ are isometric to standard 2-spheres of radius r,
- The coordinates (ϑ, φ) are standard spherical polars

General NQS metric:

$$ds^2 \quad = \quad -2u\, dz\, (dr + v\, dz) + 2|r\Theta + \overline{\beta} dr + \overline{\gamma} dz|^2$$

where $\Theta = \frac{1}{\sqrt{2}}\,(d\vartheta + \mathrm{i}\,\sin\vartheta\, d\varphi)$ and $\beta = \frac{1}{\sqrt{2}}\left(\beta^1 - \mathrm{i}\,\beta^2\right)$
$\gamma = \frac{1}{\sqrt{2}}\left(\gamma^1 - \mathrm{i}\,\gamma^2\right)$.

NQS tetrad

$$\begin{aligned} \ell &= \frac{\partial}{\partial r} - r^{-1}(\overline{\beta}\, D_v - \beta\, D_{\overline{v}}) \;=:\; \mathcal{D}_r \\ n &= u^{-1}\,(\mathcal{D}_z - v\mathcal{D}_r) \\ m &= \frac{1}{\sqrt{2}r}\left(\frac{\partial}{\partial\vartheta} - \frac{\mathrm{i}}{\sin\vartheta}\frac{\partial}{\partial\varphi}\right) \end{aligned}$$

The S^2 derivative operator ð (edth) acts on a spin-s field

$$ðη = \frac{1}{\sqrt{2}}\sin^s\vartheta\left(\frac{\partial}{\partial\vartheta} - \frac{i}{\sin\vartheta}\frac{\partial}{\partial\varphi}\right)\left(\sin^{-s}\vartheta\,\eta\right),$$

$\operatorname{div}\beta = ð\overline{\beta} + \bar{ð}\beta$ is the divergence of a vector field on S^2, and
$r\mathcal{D}_r = r\partial_r - \nabla_\beta = r\partial_r - (\beta\bar{ð} + \bar{\beta}ð)$,
$r\mathcal{D}_z = r\partial_z - \nabla_\gamma = r\partial_z - (\gamma\bar{ð} + \bar{\gamma}ð)$ are S^2-covariant operators.

Define the auxiliary variables $H,\ J,\ K,\ Q,\ Q^{\pm}$ in terms of the metric parameters:

$$
\begin{aligned}
H &= u^{-1}(2 - \operatorname{div}\beta) \\
J &= v(2 - \operatorname{div}\beta) + \operatorname{div}\gamma \\
K &= v\eth\beta - \eth\gamma \\
Q &= r\mathcal{D}_z\beta - r\mathcal{D}_r\gamma + \gamma \\
Q^{\pm} &= u^{-1}(Q \pm \eth u)
\end{aligned}
$$

Hypersurface Equations

The Einstein tensor components $G_{\ell\ell}$, $G_{\ell m}$, $G_{\ell n}$ and G_{mm} give equations involving only derivatives tangent to the null hypersurfaces:

$$
\begin{aligned}
r\mathcal{D}_r H &= \left(\tfrac{1}{2}\operatorname{div}\beta - \frac{2|\eth\beta|^2 + r^2 G_{\ell\ell}}{2-\operatorname{div}\beta}\right) H \\
r\mathcal{D}_r Q^- &= (\eth\bar{\beta} - uH)Q^- + \bar{Q}^-\eth\beta + 2\bar{\eth}\eth\beta + u\eth H - H\eth u + 2r^2 G_{\ell m} \\
r\mathcal{D}_r J &= -(1-\operatorname{div}\beta)J + u - \tfrac{1}{2}u|Q^+|^2 - \tfrac{1}{2}u\,\operatorname{div}(Q^+) - ur^2 G_{\ell n} \\
r\mathcal{D}_r K &= \left(\tfrac{1}{2}\operatorname{div}\beta + \mathrm{i}\,\operatorname{curl}\beta\right) K - \tfrac{1}{2}\eth\beta J + \tfrac{1}{2}u\eth Q^+ + \tfrac{1}{4}u(Q^+)^2 \\
&\quad + \tfrac{1}{2}ur^2 G_{mm}
\end{aligned}
$$

The NQS evolution algorithm

Begin with the primary field β on a null hypersurface $z = z_0$, and progressively solve the hypersurface constraint equations, viewed as radial ODE's for the metric parameters:

1. $G_{\ell\ell}$ gives H, and thus $u = (2 - \operatorname{div}\beta)/H$
2. $G_{\ell m}$ gives Q^-, and thus Q and Q^+
3. $G_{\ell n}$ gives J
4. G_{mm} gives K
5. Solving an elliptic system on S^2 determines γ, v from J, K
6. Determine $\frac{\partial \beta}{\partial z}$ from Q, β, γ
7. Evolve β to the next null hypersurface

Eliminating v from the definitions of J and K gives an elliptic system for the vector field γ restricted to the 2-sphere $(z, r) = const.$

$$\eth\gamma + \frac{\eth\beta}{2 - \operatorname{div}\beta} \operatorname{div}\gamma = J\frac{\eth\beta}{2 - \operatorname{div}\beta} - K\,.$$

The right hand side is known from solving the hypersurface constraint equations, so we have an elliptic system for γ. The remaining metric parameter v is then determined, by

$$v = \frac{J - \operatorname{div}\gamma}{2 - \operatorname{div}\beta}\,.$$

The primary field β is evolved using Q:

$$r\frac{\partial\beta}{\partial z} = Q + r\frac{\partial\gamma}{\partial r} + \nabla_\gamma\beta - \nabla_\beta\gamma - \gamma\,.$$

The Bianchi II (conservation law) identity ${F_{ab}}^{;b} = 0$ for a symmetric tensor F_{ab} gives equations for the components $F_{m\bar{m}}, F_{nm}, F_{nn}$ (in NP notation with $\kappa = 0$)

$$
\begin{aligned}
0 &= \mathrm{Re}\,\rho\, F_{m\bar{m}}, \\
D_\ell(F_{nm}) &= (2\rho + \bar{\rho} - 2\bar{\varepsilon})\, F_{nm} + \sigma\, F_{n\bar{m}} \\
&\quad + D_{\bar{m}} F_{m\bar{m}} + (\bar{\pi} - \tau)\, F_{m\bar{m}}, \\
D_\ell(F_{nn}) &= 2\,\mathrm{Re}(\rho - 2\varepsilon)\, F_{nn} - \mathrm{Re}\,\mu\, F_{m\overline{m}} \\
&\quad + D_m F_{n\bar{m}} + D_{\bar{m}} F_{nm} + \mathrm{Re}((2\beta + 2\bar{\pi} - \tau)\, F_{n\overline{m}}).
\end{aligned}
$$

If $\rho \neq 0$ and $F_{nm} = F_{nn} = 0$ on a boundary surface transverse to the null hypersurface, then $F_{m\bar{m}} = F_{nm} = F_{nn} = 0$ everywhere on the null hypersurface. Thus the constraint (subsidiary) equations are propagated by the evolution.

Boundary (Subsidiary) Equations

The Einstein components G_{nn}, G_{nm} yield the evolution $(\frac{\partial}{\partial z})$ relations:

$$
\begin{aligned}
r\,\mathcal{D}_z\,(J/u) &= v^2\,r\mathcal{D}_r\,(J/(uv)) + (\tfrac{1}{2}J - v)J/u \\
&\quad + 2u^{-1}|K|^2 - \nabla_{Q^+}v - \Delta v + ur^2 G_{nn} \\
r\,\mathcal{D}_z Q^+ &= \left(v\,r\mathcal{D}_r + J + \eth\bar{\gamma} - v\eth\bar{\beta}\right) Q^+ - K\bar{Q}^+ \\
&\quad + 2u^{-1} r\mathcal{D}_r(u\eth v) - (2 + \mathrm{i}\ \mathrm{curl}\,\beta)\eth v \\
&\quad + 2\bar{\eth}K + \eth J - 2u^{-1}\eth u\,J - 2ur^2 G_{nm}
\end{aligned}
$$

These equations constrain the boundary conditions for the fields J/u and Q^+. At non-boundary points they provide compatibility conditions on the z-derivatives.

Free Boundary Data

- The Hypersurface Equations require boundary data (initial conditions) for H, Q^-,J, K.
- The Boundary Equations constrain the z-evolution of the boundary data for J/u and Q^+.
- The z-evolution of β is determined everwhere from Q.
- Consequently, the boundary data for u, K are unconstrained (free).
- u determines the starting sphere for the "next" null hypersurface, hence u represents gauge freedom.
- K describes the outgoing radiation (ingoing shear) and is free geometric data.

Aspects of the Numerical Methods

- 8th order Runge-Kutta for the radial integration of the null hypersurface constraint ODEs, with 256 radial steps, rescaled to reach $\mathcal{I}^+$.
- FFT and projection to spin-weighted spherical harmonics used to minimise polar problems and to compute angular derivatives. Resolution is $L = 7, 15$ or 31.
- Preconditioned conjugate gradient method to solve the elliptic system on S^2 for γ.
- 4th order Runge-Kutta for the time evolution with timestep $\Delta z = 0.05$.

Infalling radial coordinate

Use a radial grid variable $n = 0, \ldots, n_\infty = 256$ and the Schwarzschild radius function

$$r = r(z, n) = 2M\phi^{-1}(\exp(-z/4M)\phi(f(n)/2M)),$$

where $\phi(x) := (x-1)e^x$, $x \geq 0$. Then $n = const.$ defines infalling radial curves.

Compactify $\mathcal{I}^+$ by $n_\infty - n = O(r^{-1/2})$, with

$$f(n) = f_1(\nu)/(1-\nu)^2,$$

where $\nu = n/n_\infty$, f_1 monotone on $[0, 1]$.

run_160: $|\,r\beta\,|$

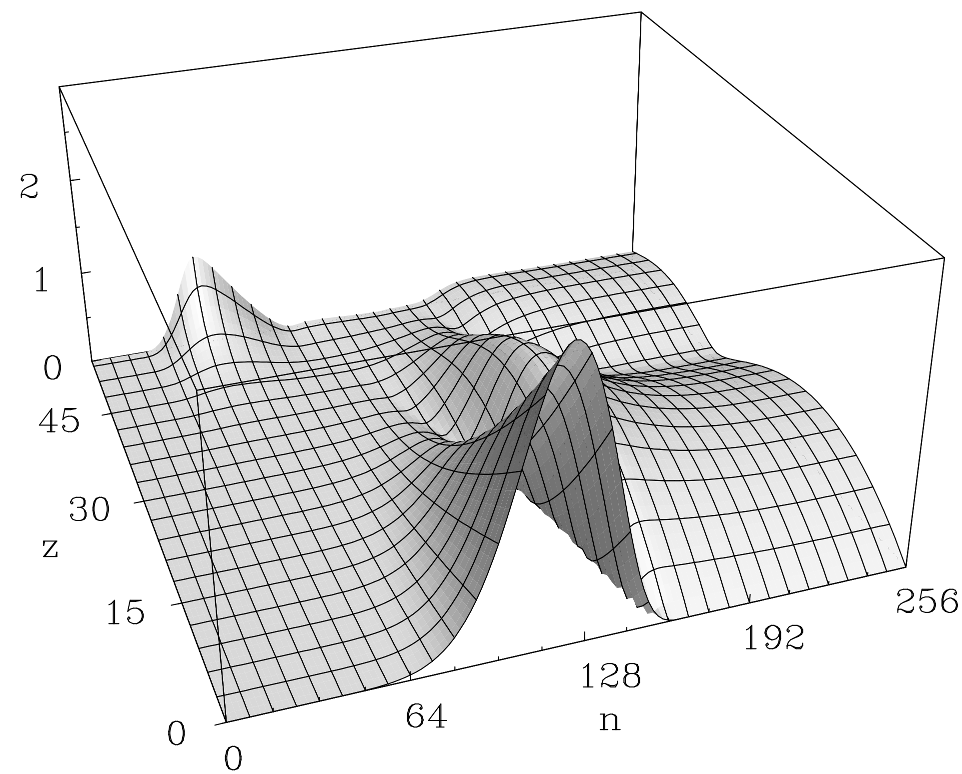

Figure 1: Evolution of $r\beta$ for $0 \leq z \leq 55$. Observe that the infalling grid tracks the dynamical evolution. $n = 0$ is the past horizon $r = 2M$, $n = 256$ is future null infinity $\mathcal{I}^+$.

Kruskal–Szekeres coordinates

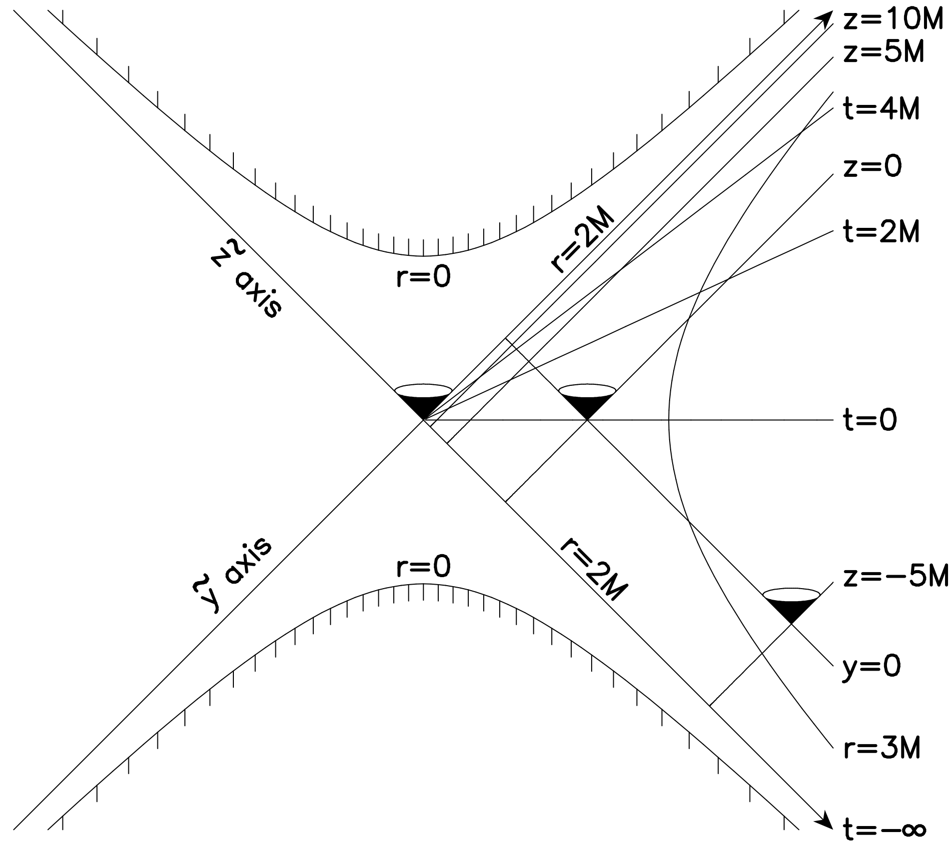

Figure 2: Schwarzschild spacetime in Kruskal-Szekeres coordinates.

Numerical convergence tests

Refine code parameters:

- radial resolution $n_\infty = 128, 256, 512, 1024$, shows 8-th order accuracy in radial integrations;
- angular resolution $L = 7, 15, 31$;
- timestep $\Delta z = 0.01, 0.05, 0.1$, shows 4-th order accuracy in timestep;

or vary initial field strength $\beta(z = 0)$:

- weak field `run_150`, with 1% of the total energy as radiation
- intermediate field `run_160`, with 20% radiation
- strong field `run_170`, with 50% radiation

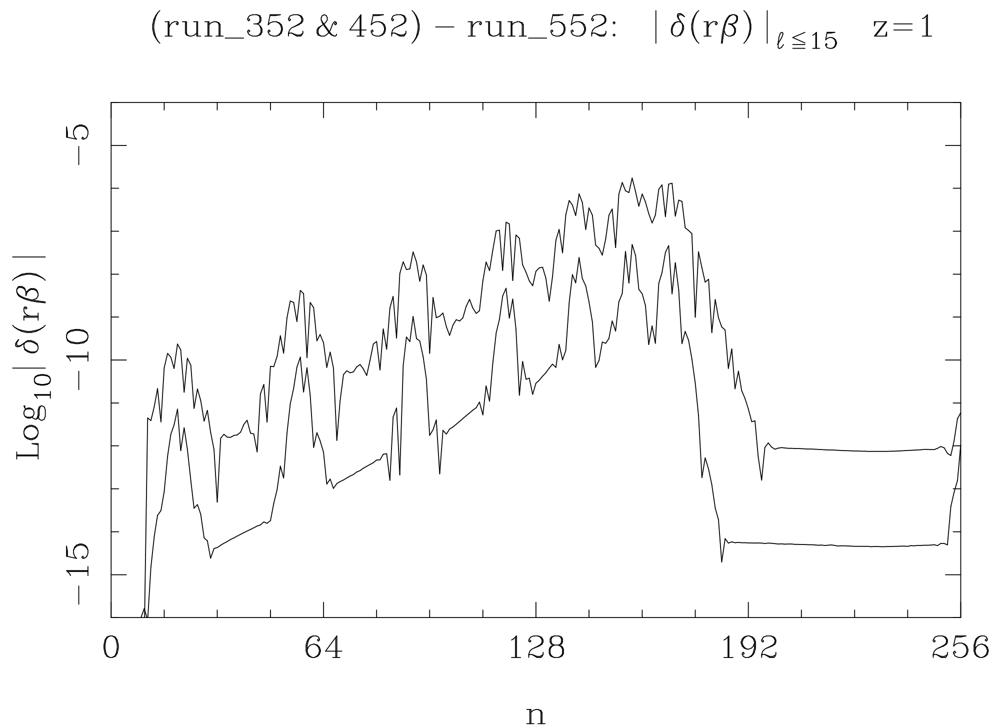

Figure 3: Convergence of β with increasing radial resolution: weak field solutions with $n_\infty = 256, 512$ compared to $n_\infty = 1024$. The error decreases by approximately a factor of 2^8 on doubling the radial resolution.

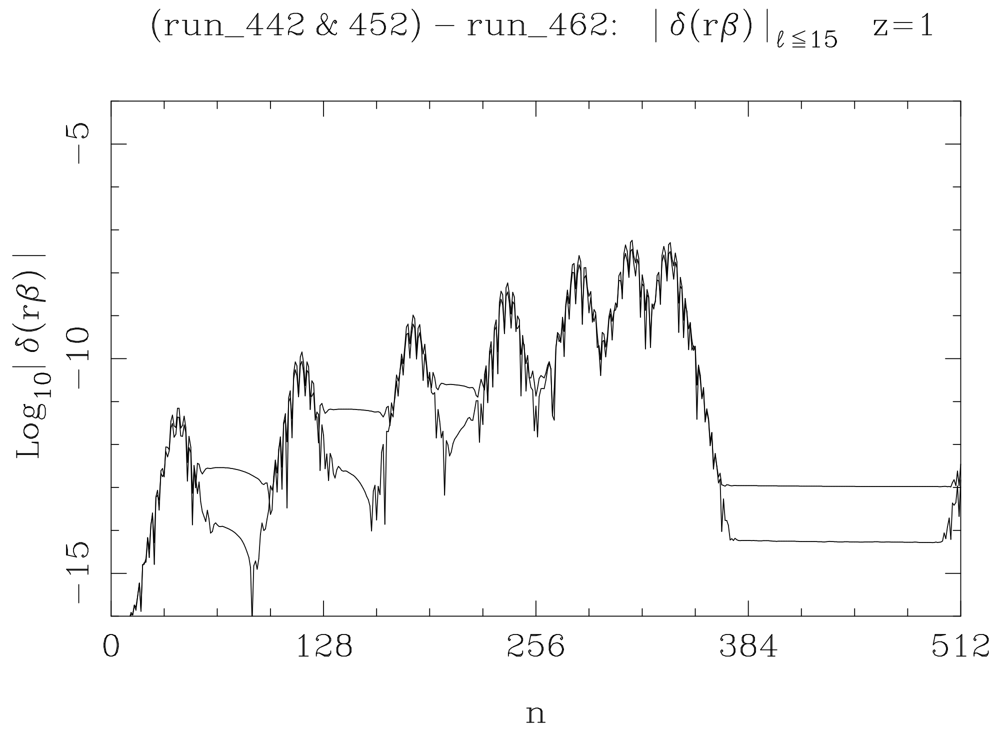

Figure 4: Convergence of β with decreasing time step: weak field solutions for $\Delta z = 0.1, 0.05$, compared against $\Delta z = 0.025$. Where the error is not dominated by the radial discretisation error, the curves show a decrease in error which is consistent with 4th order convergence.

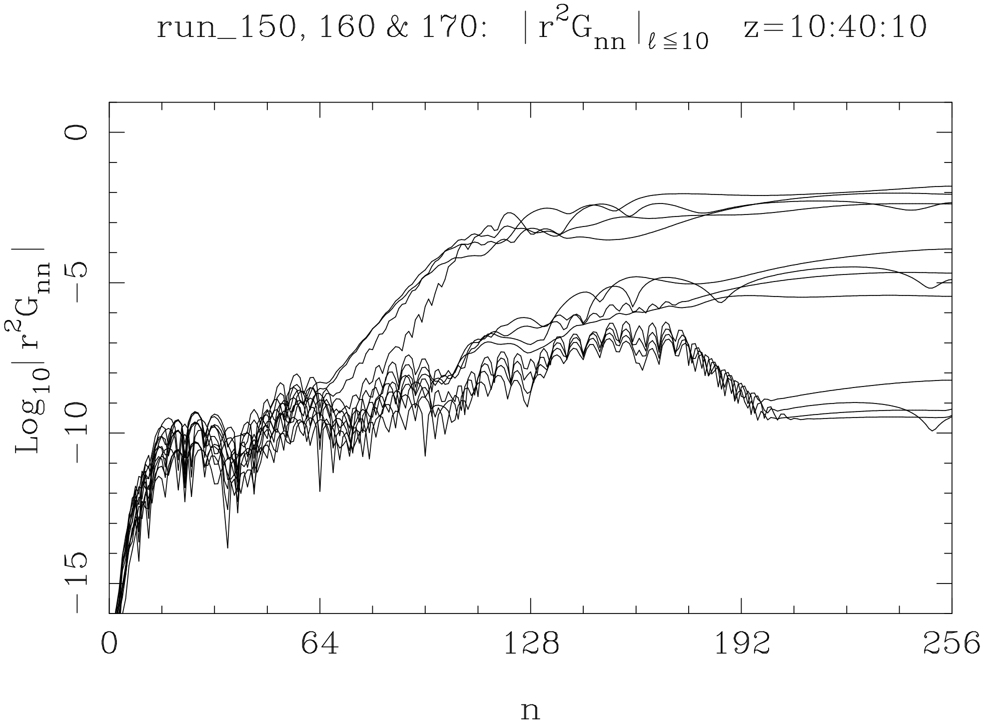

Figure 5: Effect of spectral resolution on constraint quantity $|r^2 G_{nn}|_{S^2}$ at times $z = 10, 20, 30, 40$, for strong (top 4 curves), intermediate (middle 4 curves) and weak (bottom 4 curves) fields.

Accuracy Conclusions

For the data studied (pure $l = 2$ initial β with Gaussian profile centered at $r = 20M$), the solutions are

- relatively insensitive to the timestep Δz;
- improved by increasing n_∞;
- fundamentally limited by the spectral resolution: $L = 15$ corresponds to solving the $L = 10$–truncated Einstein equations.

Geometric consistency tests

- Evaluate the constraint equations
  - $G_{nn} = G_{nm} = 0$ ("subsidiary" equations)
  - $G_{m\overline{m}}$ ("trivial" equation).
- Test the Trautman-Bondi mass loss formula (for $\frac{d}{dz} m_{Bondi}$).
- Test peeling behaviour $\Psi_k = O(r^{k-5})$ for the Weyl curvature components Ψ_k, $k = 0, \ldots, 4$.

Hawking and Bondi Mass

The Hawking mass of the $(z, r) = const.$ 2-spheres is

$$m_H(z, r) = \tfrac{1}{2} r \left(1 - \frac{1}{8\pi} \oint_{S^2} HJ \right)$$

where the integral is over the unit 2-sphere and

$$\oint_{S^2} HJ = \oint_{S^2} \frac{1}{u} (2 - \operatorname{div} \beta)(\operatorname{div} \gamma - v(2 - \operatorname{div} \beta))$$

The Bondi mass of the null hypersurface is

$$m_B(z) = \lim_{r \to \infty} m_H(r, z)$$

and the Trautman-Bondi mass-loss formula is

$$\frac{d}{dz} m_B(z) = \frac{1}{16\pi} \lim_{r \to \infty} \oint_{S^2(z,r)} H|K|^2.$$

Trautman-Bondi mass decay

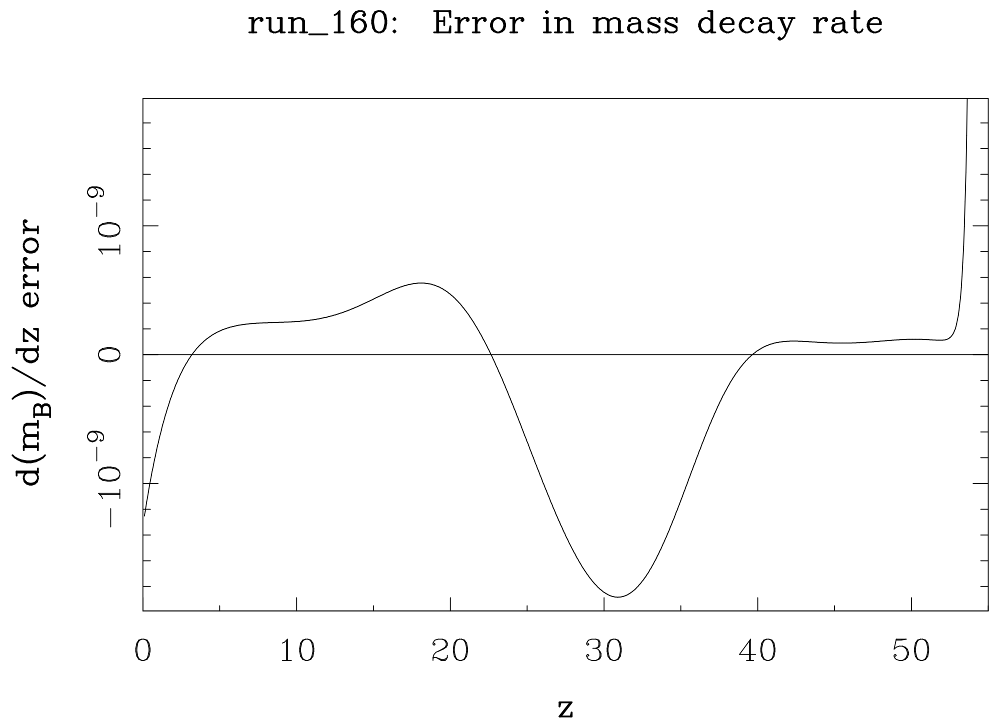

Figure 6: Difference between $\frac{d}{dz}m_B(z)$ calculated by numerical differentiation, and from the Trautman-Bondi mass-loss formula.

Example: Peeling obstruction

Under generic asymptotic behaviour ($r\beta$ bounded at scri), we find that $\Psi_0 = O(r^{-4})$, not $O(r^{-5})$ as predicted by the peeling hypothesis.

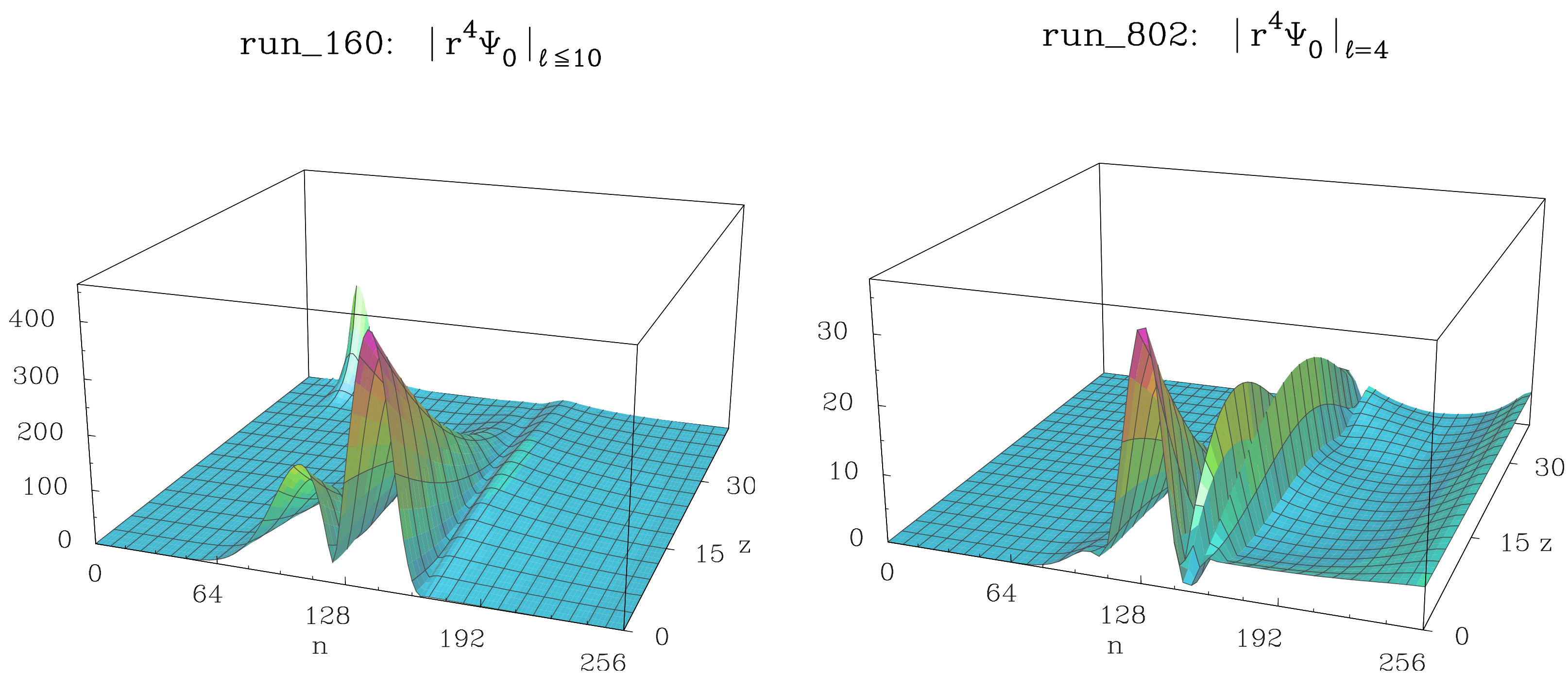

Figure 7: Comparison of $r^4\Psi_0$ shows peeling and non-peeling behaviour

Website demonstrations

1. $r\beta$ for `run_150`, $z = 0..55$ — (a) 2D plot with mpeg; (b) 3D surface plot
2. spectral decay for (a) `run_150` with $l = 0..15$, (b) `run_170` with $l = 0..10$, to estimate relative accuracy by $|l = 10| : |l = 2|$
3. Hawking mass for `run_170`
4. dm/dz for `run_170`
5. Weyl spinor $r^5\Psi_0$ for `run_160`, `run_802`